Structures of Ammonia Cluster Cations

Jong Keun Park

Department of Chemistry and Central Laboratory, Pusan National University, Pusan 609-735, Korea
Received June 11, 1999

Structures of unprotonated $[(NH_3)_n^+(n = 1\text{-}6)]$ and protonated $[NH_4^+(NH_3)_{n-1}(n = 1\text{-}6)]$ ammonia cluster cations have been optimized with ab initio Hartree-Fock (HF) and second-order Møller-Plesset (MP2)/6-31+G** levels and the harmonic vibrational frequencies have also been evaluated. In unprotonated cluster cations, NH_3^+ forms as a central core of the first ammonia solvation shell. In protonated cluster cations, NH_4^+ forms as a central core. In unprotonated dimer and trimer cations, there are two types of isomers (hydrogen-bonded and head-to-head interactions). In both cluster cations, the hydrogen-bonded isomers are more stable. In the hydrogen-bonded dimer cation, the proton transfer reaction takes place from $(NH_3\text{-}HN^+H_2)$ to $(NH_4^+\text{-}NH_2)$. But in the other unprotonated cluster cations, the proton transfer does not take place. In unprotonated pentamer and hexamer, a NH_3^+ core has both interactions in a complex. On the other hand, in unprotonated tetramer a core has only the hydrogen-bonded type combined with neutral ammonia molecules. With increasing cluster cation size, the bond lengths $[R_{(NN)}]$ between two nitrogen atoms and the distances $[R_{(N\cdots H)}]$ of the hydrogen-bond increase regularly. In the calculated infra-red absorption bands for ammonia cluster cations, the characteristic peaks of the bridged NH vibration of the hydrogen-bonded clusters appear near 2500 cm^{-1}. With increasing size, the peaks shift from 2306 cm^{-1} to 2780 cm^{-1}.

Introduction

Recently, photoionization experiments of ammonia cluster cation have been performed by electron impact,[1-4] single photon,[5-8] and multiphoton resonant[9-16] ionization spectroscopies. In these experiments, a main component is protonated ammonia cluster cations $[NH_4^+(NH_3)_{n-1}]$, while unprotonated ammonia cluster cations $[(NH_3)_n^+]$ are also detected as a by-product. The unprotonated cluster cations are found to be directly produced from neutral ammonia clusters *via* photoionization processes. On the other hand, the protonated cluster cations are found to be produced by two other mechanisms. In one mechanism, the unprotonated cluster cation is formed and then it is divided into the protonated cation and NH_2. In the other, the excited ammonia cluster $(NH_3)_{n-2}(H_3N^*\text{-}HNH_2)$ is formed from the predissociative state of an ammonia molecule in the cluster through the multiphoton absorption process and then the photoionization and photodissociation take place.

Nishi *et al.*[6,9] suggested the schematic diagram for the mechanism of unprotonated and protonated cluster cations *via* the molecular beam mass spectroscopy and electron impact methods. According to the results, the unprotonated cations $[(NH_3)_n^+]$ are very unstable. As a result, the peak intensities of unprotonated cluster cations are very weak. Potential energy representations of the multiphoton ionization processes of unprotonated and protonated cluster cations were constructed by Castleman, Jr. *et al.*[2,10-13,15] According to the ionization processes, unprotonated cluster cation is produced by the resonant enhanced multiphoton process and these cations $[(NH_3)_n^+]$ dissociate into the protonated cation $(NH_3)_{n-1}H^+ + NH_2$ along the cationic potential curves with small energy barrier. Therefore, the peaks of unprotonated cations are very weak compared with the protonated cations. On the other hand, Fuke *et al.*[16] investigated the single photon ionization experiments of unprotonated and protonated ammonia clusters without the relaxation of the intermediate excited states. In this experiment, they observed the peaks of unprotonated monomer and dimer ammonia cation.

Although the existence of unprotonated ammonia cluster cations via the photoionization and photodissociation processes have been studied by many groups,[16-30] the structures and relative stabilities of unprotonated ammonia cluster cations were rarely found. Due to the limited information on these unprotonated cluster cations, further studies of their structures and stabilities seem to be worth carrying based of the following points. i) Does the stable structures of unprotonated cations exist or not? In recent experiments, the unprotonated cluster cations $[(NH_3)_n^+]$ were rarely observed except for $n = 1$ and 2. In particular, the peak of unprotonated pentamer cation is very weak as a noise. ii) Does the proton transfer reaction takes place in all unprotonated cluster cations? Experiments by Nishi suggest that the proton transfer in all cluster cations takes place from unprotonated to protonated cations. iii) Are there any structural isomers in unprotonated cations? To answer these questions, we optimized the geometrical structures of ammonia cluster cations at the HF and MP2 levels and also analyzed the harmonic frequencies of the structures to find the local minimum of the structure.

Computational Methods

The geometrical structures of unprotonated ammonia cations $[(NH_3)_n^+(n = 1\text{-}6)]$ as well as protonated ammonia clusters $[NH_4^+(NH_3)_{n-1}(n = 1\text{-}6)]$ are fully optimized using the restricted and unrestricted Hartree-Fock (RHF, UHF)

Table 1. Bond lengths (Å) of unprotonated and protonated ammonia cluster cations

	MP2				MP2[a]				expt[b]
	$R^c_{(NN)}$	r^d_{free}	$r^e_{bridged}$	$R_{(N\cdots H)}$	$R^c_{(NN)}$	r^d_{free}	$r^e_{bridged}$	$R^f_{(N\cdots H)}$	r^d_{free}
NH_3^-		1.021							
NH_3		1.012				0.991			1.012
NH_4^-		1.023				1.012			1.032[g]
unprotonated ammonia cations									
$(NH_3)_2^-$ **(H-H)**	2.174[h]	1.014			2.204[i]	1.017[i]			
$(NH_3)_2^-$ **(H-B)**	2.791	1.022	1.068	1.723	2.770[i]	1.023[i]	1.07[i]	1.70[i]	2.8[i]
$(NH_3)_3^-$ **(H-H)**	2.504[h]	1.008							
$(NH_3)_3^-$ **(H-B)**	2.752	1.017	1.083	1.669					
$(NH_3)_4^-$	2.844		1.056	1.788					
$(NH_3)_5^-$	2.595[h]								
	2.915		1.039	1.876					
$(NH_3)_6^-$	2.738[h]								
	2.938		1.034	1.904					
protonated ammonia cations									
$(NH_4^-)(NH_3)$	2.706	1.020	1.112	1.593	2.732	1.008	1.085	1.647	
$(NH_4^-)(NH_3)_2$	2.833	1.018	1.064	1.769	2.828	1.006	1.051	1.777	
$(NH_4^-)(NH_3)_3$	2.914	1.017	1.047	1.866	2.902	1.005	1.036	1.860	
$(NH_4^-)(NH_3)_4$	2.976		1.039	1.938	2.967		1.027	1.940	
$(NH_4^-)(NH_3)_5$	2.991		1.036	1.955					

[a]Reference 32. [b]Reference 40. [c]Bond length between two nitrogen atoms of the core and ammonia monomer is noted as $R_{(NN)}$. [d]Bond length of the free N-H bond in the core NH_3^- and NH_4^- ions. [e]Bond length of the bridged N-H bond of the core. [f]Bond length of the hydrogen-bond between N and H. [g]Reference 38. [h]Bond length between two nitrogens in the head-to-head interaction. [i]Reference 17. [j]Reference 27. **H-H** indicates isomer of the head-to-head type. **H-B** indicates isomer of the hydrogen-bonded type.

and second-order Möller-Plesset perturbation (MP2; all electrons) methods with the 6-31+G** basis set. After the optimization, the harmonic vibrational frequencies are evaluated to confirm the existence of the stable structure at the HF and MP2 levels. The program used is GAUSSIAN 94.[31]

Results and Discussion

Geometrical structures of unprotonated ammonia cluster cations $[(NH_3)_n^+(n = 1\text{-}6)]$. Optimized bond lengths of unprotonated and protonated ammonia cluster cations are listed in Table 1. Optimized geometrical structures and binding energies of unprotonated ammonia cluster cations were listed in Ref. 25. The isomers of the head-to-head and the hydrogen-bonded types are noted as **H-H** and **H-B**, respectively.

The bond length between two nitrogen atoms of the core and ammonia monomer and bond length of the hydrogen-bond between N and H are noted as $R_{(NN)}$ and $R_{(N\cdots H)}$. The bond lengths of the free and bridged N-H bonds of the core NH_3^- and NH_4^- cations are indicated as r_{free} and $r_{bridged}$. The bond lengths of the free N-H bond of NH_3^-, NH_3, and NH_4^+ are listed as a reference. In ammonia cluster cations, the cations are the ion-neutral interaction complexes. As the cluster size increases, the charge-dipole interaction becomes weaker and the bond lengths $[R_{(NN)}]$ between two nitrogen atoms increase regularly. $R_{(NN)}$ of unprotonated cluster cations having a planar NH_3^+ core are shorter than those of protonated cations having a tetrahedral NH_4^+ core. With increasing cluster size, $r_{bridged}$ of the bridged N-H bond decrease stepwise, while the distances $[R_{(N\cdots H)}]$ of the hydrogen-bond increase regularly. But, by the proton transfer of the hydrogen-bond type of unprotonated dimer cation, the geometical parameters are in a irregularity.

In the head-to-head type of unprotonated dimer cation, our $R_{(NN)}$ (2.174 Å) is shorter than that (2.204 Å) of Amor *et al.*[17] calculated with the MP2/DZP level, but longer than that (2.151 Å) of Radom *et al.*[19,20] using the MP2/6-31G* level. In the hydrogen-bonded type, our $R_{(NN)}$ (2.791 Å) is longer than some results [2.770 Å from Amor *et al.*,[17] 2.776 Å from Tomoda,[21,22] and 2.783 Å from Tachibana *et al.*[18]] but shorter than others [2.877 Å from Tachikawa and Tomoda,[23] 2.80 Å from Tomoda and Kimura,[21] 2.80 Å from Cao *et al.*,[24] and 2.816 Å from Gill and Radom[19]]. In this cation, the proton-transfer takes place. As a result, the geometical parameters [$R_{(NN)}$, r_{free}, $r_{bridged}$, and $R_{(N\cdots H)}$] are in an irregular fashion.

Spectra of the calculated infra-red absorption bands of unprotonated ammonia cluster cations are drawn in Figure 1. X-axis is a frequency scale from 0 to 4000 cm^{-1} and Y-axis is a relative IR intensity scale. To compare the frequency shifts between a NH_3^+ core and complexes, the frequencies of NH_3^+ are indicated as a reference. The characteristic peaks of the symmetric and asymmetric stretching vibrational modes of the core involving the hydrogen-bonds (N···H) were drawn with black stick. The others have been indicated with a white square. In unprotonated cations, the spectra are divided into three groups. The first one is the stretching mode of the free N-H between 3000 cm^{-1} and 4000 cm^{-1}. With increasing cluster size, the stretching modes are gradu-

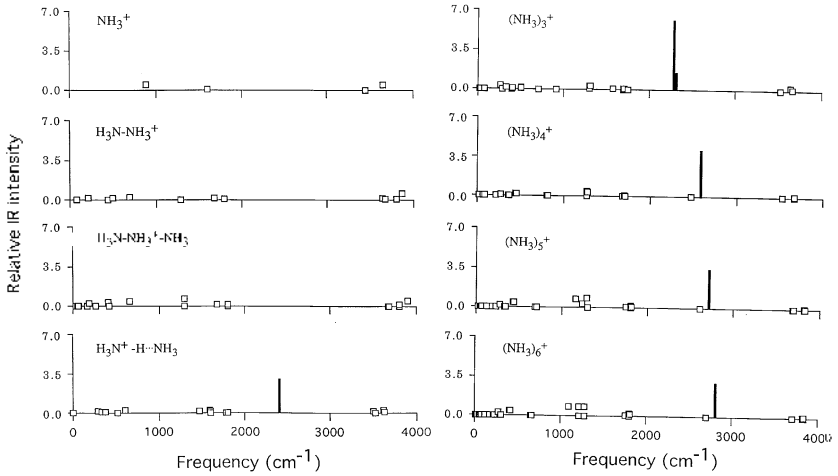

Figure 1. Stick spectra of the calculated infra-red absorption bands of unprotonated ammonia cluster cations $[(NH_3)_n (n = 1\text{-}6)]$ at the MP2/6-31+G** level. X-axis is a frequency scale from 0 to 4000 cm^{-1} and Y-axis is a relative IR intensity scale.

ally red-shifted. The second one is the bending modes between 1000 cm^{-1} and 2000 cm^{-1}. The last one is the others (such as the wagging and twist modes of the ammonia monomer unit in a complex) at the low frequency region. From dimer to hexamer, the characteristic peaks of the stretching motions of the core involving the hydrogen-bonds are shifted from 2306 to 2780 cm^{-1}. In trimer cation, two peaks with strong IR intensity are found, while in the other cations one peak is represented.

In the hydrogen-bonded type of dimer cation, the geometry has an interaction of hydrogen-bonded type between NH_4^+ and NH_2. A central NH_4^+ core of dimer cation is quite different from the NH_3^+ core of the other cations. As a result, a characteristic peak is found at 2435 cm^{-1}. The peak is red-shifted to a higher frequency region than those of the others. In unprotonated trimer cation, two hydrogens of the NH_3^+ core are hydrogen-bonded with two ammonia monomers and the third one is free. As a result, two characteristic peaks (2306 cm^{-1} and 2339 cm^{-1}) arise from the symmetric and asymmetric stretching modes of the core involving the hydrogen-bonds. A weak peak is the symmetric stretch (ν_1') of the core, while a strong peak is the asymmetric stretching modes (ν_3'').

From tetramer to hexamer cations, the NH_3^+ core has three hydrogen-bonds. Therefore, the characteristic peak of the symmetric stretching modes of the core involving the hydrogen-bonds (N···H) is inactive, that is, the intensity is zero. The asymmetric stretching mode is infrared active and the IR intensity is strong. In our frequency analysis, the symmetric and asymmetric stretching modes correspond to ν_1' and ν_3'' of ammonia monomer, respectively. Due to the symmetry of the geometrical structure from unprotonated tetramer cation to hexamer, the characteristic peaks of the calculated infra-red absorption bands are similar to each other. With increasing cluster size, the characteristic peaks are gradually blue-shifted from 2586 cm^{-1} to 2780 cm^{-1}. The stretching modes of the free N-H bond are found between 3534 cm^{-1} and 3675 cm^{-1}. The bending modes between 1269 cm^{-1} and 1711 cm^{-1} are divided into two subgroups. Between 14 cm^{-1} and 816 cm^{-1}, the other modes are found. With increasing n, the stretching bands of the free N-H and the other modes (the wagging and twist modes) change little.

In the head-to-head type of dimer and trimer cations, since the complexes have only the N-N bonds combined by the charge-dipole interactions, the characteristic peaks are not found. The stretching modes of the free N-H bonds are found between 3538 cm^{-1} and 3725 cm^{-1}. The bending modes are observed between 1105 cm^{-1} and 1660 cm^{-1} and are divided by two subgroups. The low subgroup arises from the bending as in a out-of plane motion of ammonia monomer. The higher subgroup corresponds to the inner motions of ∠HNH angle of monomer.

Geometrical structures of protonated ammonia cluster cations $[NH_4^+(NH_3)_{n-1} (n = 1\text{-}6)]$. Optimized geometrical structures of protonated ammonia cluster cations are drawn in Figure 2. NH_4^+ is located at a central core of protonated cluster cations. With increasing cluster size, four hydrogen atoms of the NH_4^+ core are gradually combined with the neutral ammonia molecule to make the hydrogen-bonded complexes. Our optimized geometrical structures of the protonated cations are in good agreement with the other theoretical[32-34] and experimental[35-41] results. In protonated dimer cation, the geometrical structure with C_{3v}-symmetry is optimized at the MP2 level, that is, a nitrogen atom of neutral ammonia is bound to a hydrogen of the NH_4^+ core. The hydrogen atom between the monomers is located at one side. Meanwhile, the structure with D_{3d}-symmetry is found to be a transition state with an imaginary frequency in the MP2 frequency analysis. At the CCSD(T) level, the geometrical structure with D_{3d}-symmetry can not be optimized. But, Price *et al.*[35] have concluded that a stable geometrical structure of protonated dimer cation is D_{3d}-symmetry.

In protonated trimer cation, two hydrogens of the core interact with two monomers and two hydrogens are free. In tetramer cation, three ammonia monomers are bonded to each of the hydrogen atoms of the central core. In pentamer cation, each of the hydrogen atoms of the central NH_4^+ core combines with four ammonia monomers. That is, the first

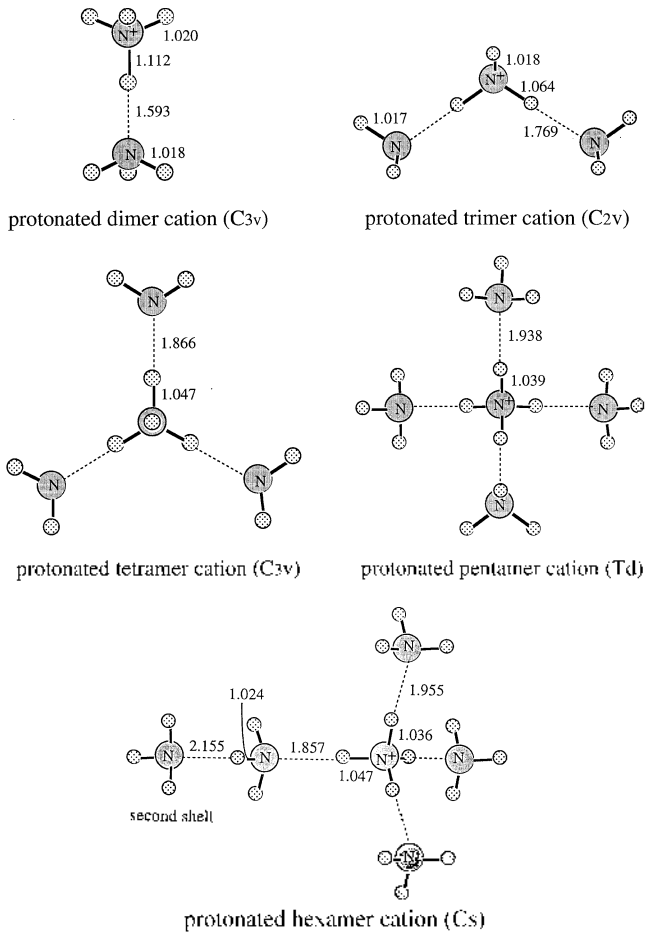

Figure 2. Optimized geometrical structures of protonated ammonia cluster cations $[NH_4^+(NH_3)_{n-1}(n = 1\text{-}6)]$ at the MP2/6-31+G** level.

ammonia solvation shell is completed. Kassab and Evleth[32] optimized the geometrical structure with C_{3v}-symmetry, using the RHF/4-31G** level, while Hirao *et al.*[33] optimized the structure with T_d-symmetry, using the RHF/6-31G** level. Experimentally, Echt *et al.*[39] observed a peak with strong intensity for the pentamer cation. They concluded that the strong intensity results from a stable geometrical structure $[NH_4(NH_3)_4]$ due to a closed solvation shell.

In protonated hexamer cation, the sixth ammonia molecule is located at the second ammonia solvation shell, that is, a nitrogen of the sixth ammonia molecule is bound to a hydrogen of the fifth ammonia (bridged ammonia) of the first ammonia shell. The distance [$R_{(N\cdots H)}$ = 2.155 Å] of the hydrogen-bond between the sixth ammonia and the bridged ammonia of the first shell is longer than that (1.857 Å) between the core and the bridged ammonia. The distance (1.857 Å) of the hydrogen-bond between the bridged ammonia and the core is shorter than that (1.955 Å) between the free ammonia and the core. And the distance (1.024 Å) of a bridged N-H bond of the bridged ammonia is shorter than that (1.047 Å) of a bridged N-H bond of NH_4^+.

Optimized bond lengths of protonated ammonia cluster cations are listed in Table 1. With increasing cluster cation size, $R_{(N\cdots N)}$ and $R_{(N\cdots H)}$ of intermonomer increase regularly. As shown in Ref. 25, the binding energies decrease stepwise with size. In protonated hexamer cations, although the sixth monomer is located at the second shell, the binding energy decreases in a regular fashion.

Spectra of the calculated infra-red absorption bands of protonated ammonia cluster cations are drawn in Figure 3. The notations are the same as in Figure 1. To compare the frequency shifts between a NH_3^+ core and complexes, the frequencies of NH_3 and NH_4^+ are indicated as a reference. With increasing cluster sizes, the characteristic peaks of the symmetric and asymmetric stretching modes of the core having the hydrogen-bond are found to be blue-shifted regularly. While, the stretching modes of the free N-H bond of the core are gradually red-shifted. And the bending and the wagging and twist modes change little.

In protonated dimer cations with C_{3v}-symmetry, a characteristic peak made from the symmetric stretching mode of the core is found at 2033 cm^{-1}. The stretching modes of the free N-H bond are found between 3503 cm^{-1} and 3656 cm^{-1}. The bending modes between 1321 cm^{-1} and 1807 cm^{-1} and

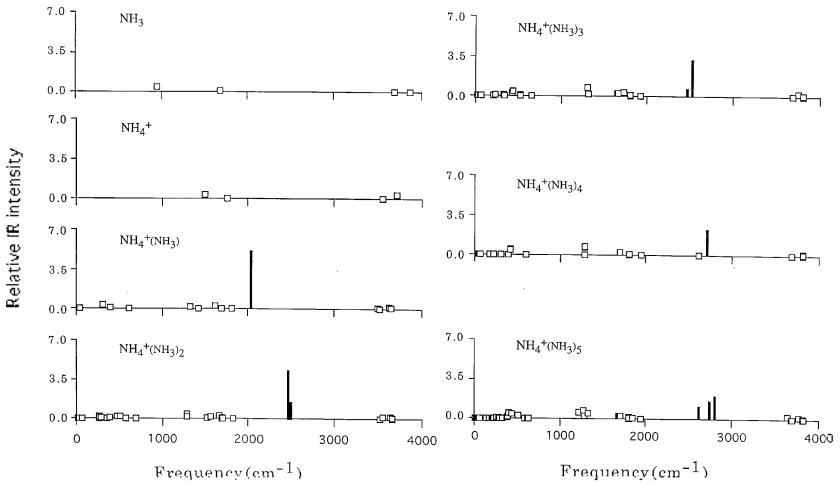

Figure 3. Stick spectra of the calculated infra-red absorption bands of protonated ammonia cluster cations $[NH_4(NH_3)_{n-1}(n = 1\text{-}6)]$ at the MP2/6-31+G** level. X-axis is a frequency scale from 0 to 4000 cm^{-1} and Y-axis is a relative IR intensity scale.

the other modes (the wagging and twist modes) at low frequency region are found. In trimer cation, two hydrogens of NH_4 are hydrogen-bonded with two ammonia monomers and the others are free. As a result, two characteristic peaks (2500 cm^{-1} and 2518 cm^{-1}) are made by the symmetric and asymmetric stretching modes of the core. In Schwarz's experiment,[36] two peaks are observed to be broad and weak between 2400 cm^{-1} and 2600 cm^{-1}, respectively.

In protonated tetramer, three vibrational modes are observed from the symmetric stretching vibrational mode (ν_1') of the core and two asymmetric stretching modes formed from the free N-H bond (ν_3') of the core and from the hydrogen-bond (ν_3''). In the experiment by Price *et al.*, the frequencies of the symmetric and asymmetric stretching modes (ν_1', ν_3'') are 2660 cm^{-1} and 2692 cm^{-1}, respectively. The frequency of ν_3' with strong intensity is 2615 cm^{-1}. Meanwhile, in our frequency of the tetramer cation, two characteristic peaks are analyzed from the symmetric and asymmetric stretching modes. One (2627 cm^{-1}) is weak peak, which is the symmetric stretching mode (ν_1') of the core. The other (2670 cm^{-1}) is a strong peak, which is made from the degeneracy of the asymmetric stretching modes (ν_3', ν_3''). Our results are similar to those of Schwarz.[36]

In protonated pentamer, the first solvation shell of the core cation is completed. Therefore, the characteristic peak of the symmetric stretching modes of the core is inactive. The asymmetric stretching mode is infrared active and the IR intensity is strong. Our frequency of the asymmetric stretching is 2762 cm^{-1}. By the experimental results of Price *et al.*,[35] and Schwarz[36] the frequencies of the asymmetric stretching modes are found at 2867 cm^{-1} and 2865 cm^{-1}, respectively.

In protonated hexamer cation, the structure of C_s-symmetry has three different environmental hydrogen-bonds. As a result, three characteristic peaks are made from the three different stretching modes. The middle one (2735 cm^{-1}) is made from the symmetric stretching mode of the core. This peak has weak intensity. The lowest one (2650 cm^{-1}) is made from the asymmetric stretching mode of the core due to the hydrogen-bond between a bridged monomer and the sixth monomer. This peak first appeared at hexamer. By the experimental results,[35] the intensity of this peak greatly increases as the number of solvent molecules at the second shell increases, and the position of this peak greatly blue-shifts as the number of solvent molecules at the second shell increases. The highest one (2783 cm^{-1}) is made from the asymmetric stretching mode of the core due to the hydrogen-bond between the core and the bridged monomer in the first shell. The intensity of this peak is influenced on the interaction of the hydrogen-bond. The spectra of the calculated infra-red absorption bands of protonated ammonia cluster cation are in good agreement with the experimental results.[35-37]

Conclusions

We optimized the geometrical structures of unprotonated $[(NH_3)_n^-(n = 1\text{-}6)]$ and protonated $[NH_4^+(NH_3)_{n-1}(n = 1\text{-}6)]$ ammonia cluster cations and evaluated the harmonic vibrational frequencies. In unprotonated cations, a planar NH_3^- ion is located at a central core of the first ammonia solvation shell. In dimer and trimer cations, there are two types of isomers, like hydrogen-bonded and head-to-head interactions. In both isomers, the hydrogen-bonded complex is more stable. In hydrogen-bonded dimer cation, the proton transfer reaction takes place from (H_3N-HN^-H_2) to (NH_4^+-NH_2). But in the other unprotonated cluster cations, proton transfer does not take place. In pentamer and hexamer, the central NH_3^- ion hydrogen-bonds with the ammonia monomers and simultaneously faces to the other NH_3 through the head-to-head interaction in a complex. On the other hand, in unprotonated tetramer cations the hydrogen-bonded isomer exists only. With increasing cluster size, the charge-dipole interaction is weaker. The bond lengths [$R_{(N\text{-}N)}$] between two nitrogen atoms and the distances [$R_{(N\cdots H)}$] of the hydrogen-bond increase regularly. And the binding energies of cluster cations decrease stepwise.

In the calculated infra-red absorption bands for ammonia cluster cations, the characteristic peaks of the hydrogen-bonded clusters appear near 2500 cm^{-1}. With increasing n, the peaks are shifted from 2306 cm^{-1} to 2780 cm^{-1}. In unprotonated dimer cation with a NH_4^- core, the peak is red-shifted more than that of trimer.

In protonated ammonia cluster cations, a NH_4^- ion forms a central core of the first ammonia solvation shell clusters. All clusters are the hydrogen-bonded complexes and the proton- and charge-transfer do not take place. The first ammonia solvation shell is completed with the pentamer configuration. In the protonated cations, the peaks of the stretching mode of the core having the hydrogen-bonds red-shift from 2030 cm^{-1} to 2783 cm^{-1} with increasing n. In protonated hexamer cation with the second ammonia solvation shell, three characteristic peaks are found at the frequency region.

Acknowledgment. The author thanks Professor Sun for the invaluable help.

References

1. Lifshitz, C.; Louage, F. *J. Phys. Chem.* **1989**, *93*, 5633.
2. Stephan, K.; Futrell, J. H.; Peterson, K. I.; Castleman, A. W., Jr.; Wager, H. E.; Djuric, N.; Mark, T. D. *Int. J. Mass Spectrom. Ion Phys.* **1982**, *44*, 167.
3. Buck, U.; Lauenstein, Ch. *J. Chem. Phys.* **1990**, *92*, 4250.
4. Gellene, G. I.; Porter, R. F. *J. Phys. Chem.* **1984**, *88*, 6680.
5. Ceyer, S. T.; Tiedemann, P. W.; Mahan, B. H.; Lee, Y. T. *J. Chem. Phys.* **1979**, *70*, 14.
6. Shinohara, H.; Nishi, N.; Washida, N. *J. Chem. Phys.* **1985**, *83*, 1939.
7. Kaiser, E.; de Vries, J.; Steger, H.; Menzel, C.; Kamke, W.; Hertel, I. V. *Z. Phys. D* **1991**, *20*, 193.
8. Kamke, W.; Herrman, R.; Wang, Z.; Hertel, I. V. *Z. Phys. D* **1988** *10*, 491.
9. Shinohara, H.; Nishi, N. *Chem. Phys. Lett.* **1987**, *141*, 292.
10. Castleman, A. W., Jr.; Tzeng, W. B.; Wei, S.; Morgan, S. *J. Chem. Soc. Faraday Trans* **1990**, *86*, 2417.

11. Wei, S.; Purnell, J.; Buzza, S. A.; Stanley, R. J.; Castleman, A. W., Jr. *J. Chem. Phys.* **1992**, *97*, 9480.
12. Wei, S.; Purnell, J.; Buzza, S. A.; Castleman, A. W., Jr. *J. Chem. Phys.* **1993**, *99*, 755.
13. Purnell, J.; Wei, S.; Buzza, S. A.; Castleman, A. W., Jr. *J. Phys. Chem.* **1993**, *97*, 12530.
14. Misaizu, F.; Houston, P. L.; Nishi, N; Shinohara, H.; Kondow, T.; Kinoshita, M. *J. Chem. Phys.* **1993**, *98*, 336; *J. Phys. Chem* **1989**, *93*, 7041.
15. Buzza, S. A.; Wei, S.; Purnell, J.; Castleman, A. W., Jr. *J. Chem. Phys.* **1995**, *102*, 4832.
16. Fuke, K.; Takasu, R. *Bull. Chem. Soc. Jpn.* **1995**, *68*, 3309.
17. Ben Amor, N.; Maynau, D.; Spiegelmann, F. *J. Chem. Phys.* **1996**, *104*, 4049.
18. Tachibana, A.; Kawauchi, S.; Kurosaki, Y.; Yoshida, N.; Ogihara, T.; Yamabe, T. *Chem. Phys.* **1994**, *182*, 185.; *J. Phys. Chem.* **1991**, *95*, 9647.
19. Gill, P. M. W.; Radom, L. *J. Am. Chem. Soc.* **1988**, *110*, 4931.
20. Bouma, W. J.; Radom, L. *J. Am. Chem. Soc.* **1985**, *107*, 345.
21. Tomoda, S.; Kimura, K. *Chem. Phys. Lett.* **1985**, *121*, 159.
22. Tomoda, S. *Chem. Phys.* **1986**, *110*, 431.
23. Tachikawa, H.; Tomoda, S. *Chem. Phys.* **1994**, *182*, 185.
24. Cao, H. Z.; Evleth, E. M.; Kassab, E. *J. Chem. Phys.* **1984**, *81*, 1512.
25. Park, J. K. *Bull. Korean Chem. Soc.* **1999**, *20*, 592.
26. Park, J. K.; Iwata, S. *J. Phys. Chem.* **1997**, *101*, 3613.
27. Buck, U.; Meyer, H.; Nelson, D., Jr.; Fraser, G.; Klemperer, W. *J. Chem. Phys.* **1988**, *88*, 3028.
28. Posey, L. A.; Guettler, R. D.; Kirchner, N. J.; Zare, R. N. *J. Chem. Phys.* **1994**, *101*, 3772.
29. Ganghi, N.; Wyatt, J. L.; Symons, M. C. R. *J. Chem. Soc. Chem. Commun.* **1986**, 1424.
30. Tomoda, S.; Suzuki, S.; Koyano, I. *J. Chem. Phys.* **1988**, *89*, 7268.
31. Frish, M. J.; Trucks, G. W.; Head-Gordon, M. H.; Gill, P. M. W.; Wong, M. W.; Foresman, J. B.; Johnson, B. G.; Schlegel, H. B.; Robb, M. A.; Replogle, E. S.; Gomperts, R.; Andres, J. L.; Raghavachari, K.; Binkley, J. S.; Gonzalez, C.; Martin, R. L.; Fox, D. J.; Defrees, D. J.; Baker, J.; Stewart, J. J. P.; Pople, J. A. *Gaussian 94*; Gaussina Inc.; Pittsburgh, PA, 1995.
32. Kassab, E.; Evleth, E. M. *J. Am. Chem. Soc.* **1987**, *109*, 1653.
33. Hirao, K.; Fujikawa, T.; Konishi, H.; Yamabe, S. *Chem. Phys. Lett.* **1984**, *104*, 184.
34. (a) Park, J. K. *J. Chem. Phys.* **1997**, *107*, 6795. (b) Park, J. K. *J. Chem. Phys.* **1998**, *109*, 9753.
35. Price, J. M.; Crofton, M. W.; Lee, Y. T. *J. Phys. Chem.* **1991**, *95*, 2182.
36. Schwarz, H. A. *J. Chem. Phys.* **1980**, *72*, 284.
37. Ichihashi, M.; Yamabe, J.; Murai, K.; Nonose, S.; Hirao, K.; Kondow, T. *Structures and Dynamics of Clusters*; Kondow, T.; Kaya, K.; Terasaki, A., Eds.; Universal Academy Press: Tokyo, 1995; Vol. 16, pp 389-395.
38. Fuke, K.; Takasu, R.; Misaizu, F. *Chem. Phys. Lett.* **1994**, *229*, 597.
39. Echt, O.; Morgan, S.; Dao, P. D.; Stanley, R. J. ; Castleman, A. W., Jr. *Phys. Chem.* **1984**, *88*, 217.
40. Keesee, R. G.; Castleman, A. W., Jr. *J. Phys. Chem. Ref. Data* **1986**, *15*, 1011.
41. Wei, S.; Tzeng, W. B.; Castleman, A. W., Jr. *J. Chem. Phys.* **1990**, *92*, 332; **1990**, *93*, 2506.